Available online at www.sciencedirect.com
ScienceDirect
Journal of Sound and Vibration 302 (2007) 936–950
JOURNAL OF SOUND AND VIBRATION
www.elsevier.com/locate/jsvi

Stochastic spur gear dynamics by numerical path integration

A. Naess[a,*], F.E. Kolnes[b], E. Mo[c]

[a]Centre for Ships and Ocean Structures, Department of Mathematical Sciences, Norwegian University of Science and Technology, Trondheim, Norway
[b]Programme for Industrial Mathematics, Department of Mathematical Sciences, Norwegian University of Science and Technology, Trondheim, Norway
[c]Department of Mathematical Sciences, Norwegian University of Science and Technology, Trondheim, Norway

Received 10 November 2005; received in revised form 12 December 2006; accepted 19 December 2006
Available online 16 February 2007

Abstract

In this paper the method of numerical path integration is applied to investigate the dynamics of a model of a pair of meshing spur gears. Our approach is based on the observation that the dynamics of a nonlinear mechanical system excited by a deterministic loading process can, to a large extent, be characterized by the response obtained by adding a small white noise to the loading. By this, the response can be expressed as a Markov diffusion process, which makes available the powerful toolbox of stochastic analysis, in particular the path integration method.

1. Introduction

Investigating the dynamics of a pair of meshing spur gears presents a challenge inasmuch as a realistic model of such a system is strongly nonlinear and usually involves a nonsmooth backlash function. The inadequacy of a linear model for predicting the dynamics of gear pairs has been clearly demonstrated by experimental studies [1,2]. The reader is referred to Ref. [3] for a literature review of published approaches to the study of the dynamics of gear pairs, see also Refs. [4,5]. A common feature of all these approaches is to study the response of the gear system to harmonic forcing or to forcing consisting of a sum of harmonic components. This leads to a strictly deterministic analysis. An early effort to include uncertain or stochastic effects is presented in Ref. [6]. A stochastic analysis may be justified on the grounds that there is never a perfectly harmonic variation of the forcing terms. However, another view on this issue could be that a complementary stochastic analysis may in fact disclose many of the characteristic features of the deterministic model, and by that provide further insight into the dynamics of gears. This can be achieved by adding a small white noise to the harmonic forcing term. In this way the theory of stochastic differential equations (SDE) and, in particular, the numerical path integration (PI) method becomes applicable [7,8]. As will be demonstrated in this paper, this kind of stochastic analysis may be very helpful in understanding the underlying deterministic dynamics. Pioneering work on the application of stochastic methods to the

*Corresponding author. Tel.: +47 73 59 47 00; fax: +47 73 59 47 01.
E-mail address: arvid.naess@bygg.ntnu.no (A. Naess).

0022-460X/$ - see front matter © 2007 Elsevier Ltd. All rights reserved.
doi:10.1016/j.jsv.2006.12.017

study of rattling in meshing gears can be found in Refs. [9,10]. Our work bears significant resemblance to these early efforts, but differs in some important aspects concerning the adopted dynamic model of the gear system.

Gear systems have a vast area of application in mechanical installations. The understanding of the dynamics behind such systems is far from complete and is complicated by the fact that the systems contain a backlash nonlinearity. Installations containing gears usually have an audible noise which in most cases is undesirable. Understanding how this noise is generated in order to be able to construct quieter systems is part of the motivation for studying models for these systems. The dynamic model that will be adopted in this paper is discussed in Ref. [11].

The scope of the work we present here is mainly of an exploratory nature, where only a very limited number of problems have been addressed. The main purpose has been to investigate and illustrate the applicability of the PI method in disclosing the dynamic characteristics of gear systems.

2. A model of meshing spur gears

2.1. A nonsmooth dynamic model

The system considered has two meshing spur gears G_1 and G_2 in the same plane where G_1 is driven by a motor providing constant torque F and G_2 is only influenced by the interaction of the gears. The gears and shafts are, for simplicity, assumed to have the same moment of inertia I, friction coefficient d and radius r.

To prevent the system from jamming, the gaps between the teeth are slightly larger than the width of the teeth, giving rise to a backlash region. There are now three possibilities for the state of the system. Ideally the gears are in contact such that G_1 drives G_2. The system may also be operating in free-play when there is no contact between the teeth. The last possibility is that the gears make contact "on the other side" so that G_2 actually drives G_1. The difference between the gap size and the width of the teeth is 2β, specifying the total gear backlash. It is believed that the audible noise occurs as the teeth make contact exiting the free-play state.

Due to imperfections in the mounting, the gears are assumed to have a small eccentricity which results in a time varying vertical displacement as the gears rotate, denoted by $e_\alpha(t)$, $\alpha = 1, 2$. The system is illustrated in Fig. 1, where the teeth geometry has been simplified for ease of representation.

Denoting the angular displacement of the driving gear by θ_1 and that of the free gear by θ_2 and the interaction between them by $b(\theta_1, \theta_2, t)$, it is obtained that

$$\begin{aligned} I\ddot{\theta}_1 + d\dot{\theta}_1 + rb(\theta_1, \theta_2, t) &= F, \\ I\ddot{\theta}_2 + d\dot{\theta}_2 - rb(\theta_1, \theta_2, t) &= 0. \end{aligned} \tag{1}$$

Here b can be expressed in terms of a backlash function B as

$$b(\theta_1, \theta_2, t) = k(t)B(\theta_1 - \theta_2 + e(t)), \tag{2}$$

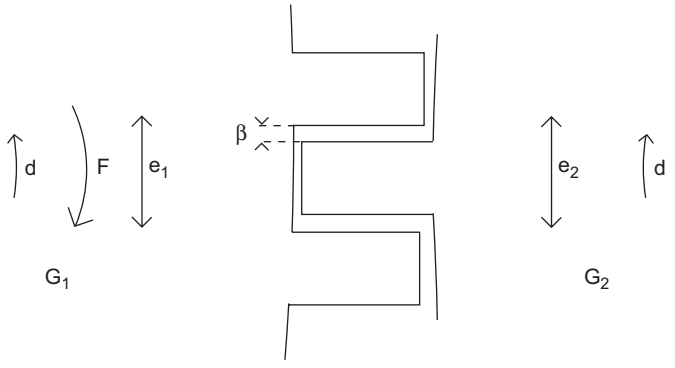

Fig. 1. Schematic illustration of the meshing gears.

where B is given as

$$B(y) = \begin{cases} y - \beta, & y > \beta, \\ 0, & |y| \leqslant \beta, \\ y + \beta, & y < -\beta \end{cases} \tag{3}$$

and $e(t) = e_1(t) + e_2(t)$. $B(\cdot)$ can be seen in Fig. 2. $k(t)$ denotes the instantaneous mesh stiffness of the gear pair, which varies periodically, see Refs. [5,12–14]. The influence of the eccentricity $e(t)$ on $k(t)$ is neglected. For the simplified model we have adopted in this paper the gear mesh stiffness is assumed to be constant, that is, $k(t) = \kappa = \text{constant}$. Linear damping has been assumed, which is the most commonly adopted model [5], while in some cases it would have been relevant to also include, e.g. dry friction. Further, it may sometimes lead to a more realistic model if a certain degree of energy loss is associated with the transition between the free-play and the contact phase [15]. Since this effect is commonly neglected in the analysis of gear dynamics, we have chosen to do the same. However, gear models obtained by including such elements can also be studied by the method presented in this paper.

In the limit when $\kappa \to \infty$ the case of perfectly elastic impacts is reached. For a review of the literature on random vibrations with impacts, cf. Ref. [16]. However, for finite κ our dynamic model is different from that of the classical vibro-impact systems. The similarity lies in the strongly nonlinear and nonsmooth backlash restoring force function $B(\cdot)$. Some authors refer also to such systems as being of (soft) vibro-impact type [5,16]. For a discussion of the dynamics of vibro-impact and strongly nonlinear dynamic systems, cf. Ref. [17].

By assuming the gears to be running at approximately constant angular speed Ω and using that, upon this assumption, the energy put into the system by the forcing should equal the energy dissipated by the interaction and friction, it is obtained that

$$\begin{aligned} d\bar{\dot{\theta}}_1 + r\bar{b} &= F, \\ d\bar{\dot{\theta}}_2 - r\bar{b} &= 0, \end{aligned} \tag{4}$$

where the overbar denotes the time average. Assuming an average rotational speed $2\pi\Omega$, adding the two equations yields

$$F = 4\pi \mathrm{d}\Omega. \tag{5}$$

This system may be transformed into a single degree of freedom system by a change of variable

$$\Theta(t) - e(t) = \theta_1(t) - \theta_2(t). \tag{6}$$

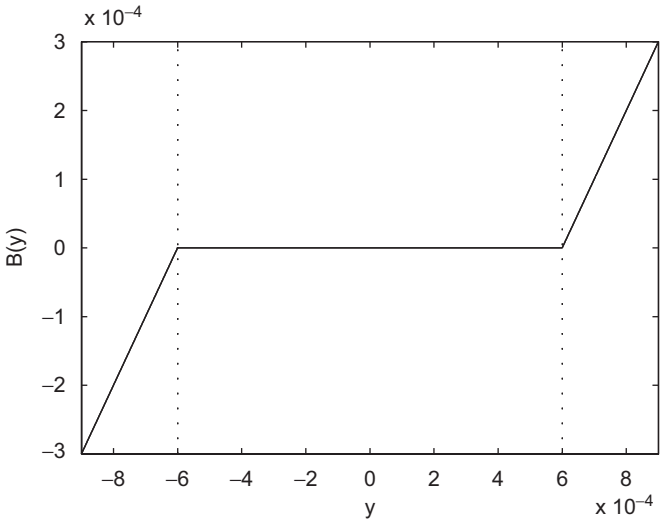

Fig. 2. The backlash function B for $\beta = 6 \times 10^{-4}$.

Now the system Eq. (1) becomes

$$\ddot{\Theta} + \frac{d}{I}\dot{\Theta} + \frac{2r\kappa}{I}B(\Theta) = \frac{F}{I} + \frac{d}{I}\dot{e} + \ddot{e}. \tag{7}$$

It is assumed [11] that the eccentricity is sinusoidal with period corresponding to the rotation of the gears, so that the right-hand side can be approximated as

$$\frac{F}{I} + \frac{d}{I}\dot{e} + \ddot{e} = \frac{F}{I} + \varepsilon\cos(2\pi\Omega t). \tag{8}$$

The substitution $\tilde{t} = \Omega t$ makes the time dimensionless, and renaming the coefficients yields the nondimensionalized single degree of freedom equation of motion

$$\ddot{\Theta} + \delta\dot{\Theta} + 2\kappa B(\Theta) = 4\pi\delta + \varepsilon\cos(2\pi\tilde{t}), \tag{9}$$

which will be the main focus of this study. Here the dot denotes differentiation w.r.t. $\tilde{t}$. The system equation may be rewritten as a system of first-order equations

$$\begin{aligned} \dot{\Theta} &= \Phi, \\ \dot{\Phi} &= 4\pi\delta + \varepsilon\cos(2\pi\tilde{t}) - \delta\Phi - 2\kappa B(\Theta). \end{aligned} \tag{10}$$

Appropriate values of the pertinent nondimensionalized parameters are given in Table 1.

2.2. Vibrational aspects

To simplify the analysis, we assumed that the mesh stiffness, which is a periodically time-varying function, could be approximated by a constant. Retaining the time varying mesh stiffness gives rise to a parametric vibration problem [18]. And, generally, the variation of meshing stiffness is a major source of vibration in gears. One of the reasons for this is the observed strong interaction between the time-varying mesh stiffness and the gear backlash [19]. In principle, the numerical PI method described in the present paper is able to cope with the case of time-variant meshing stiffness without having to simplify the nonsmooth backlash function already included in our model. It is therefore desirable to apply the PI method also to this more general and difficult case. This will be pursued in future work.

3. Deterministic solutions

As a basis for studying the system with random perturbation, it is of interest to get a certain understanding of the underlying deterministic behaviour. Some research on this topic exists [11,3], but many aspects are not understood.

The focus of this work is the stochastic gear model, and the objective of this section is to get a basic understanding of the structures that are believed to influence a noisy gear model. As suggested in Ref. [3], the deterministic model has harmonic-, subharmonic- and chaotic solutions, but investigations into the existence and stability of these are outside the scope of this paper.

In order to limit the range of possible solutions, the dimensionless parameters of Table 1 will be thought of as a ''realistic'' case, and the parameters of interest will be varied around these.

Table 1
Nondimensionalized parameters

Parameter	Typical value
β	$4 - 8 \times 10^{-4}$
δ	3×10^{-4}
ε	1×10^{-4}
κ	110

The forcing is periodic, hence it is expected that there are initial conditions and parameter values resulting in periodic Θ. As in Ref. [11] the notation $P(m, n^+, n^-)$ is introduced. Here m is the periodicity of the solution, that is $\Theta(t) = \Theta(t+m)$, n^+ is the number of times per period the system hits the upper boundary $\Theta = \beta$ and n^- the number of times per period the system hits the lower boundary $\Theta = -\beta$. Other types of solutions Θ may also exist.

When $\kappa \to \infty$ explicit solutions may be derived [11]. For the realistic parameter values such solutions are not available, but stroboscopic plots suggest there are periodic solutions for these parameter values as well.

The bifurcation theory of this system is a topic of ongoing research. It is well beyond the scope of this work to make a detailed study of these phenomena.

To gain insight into the nature of the deterministic solutions, a range of numerical simulations were carried out for different initial and parameter values to get an idea of which solutions exist for the parameters in Table 1.

Phase space plots for $m = 1$ and 2 are shown in Fig. 3. A $P(1, 1, 0)$-solution exists, but for $m > 1$, the orbits hit the other boundary.

Decreasing the damping parameter from $\delta = 3.0 \times 10^{-4}$ to $\delta = 0.5 \times 10^{-4}$, leads to the phase space plots shown in Fig. 4.

The study of the deterministic system revealed that the existence of solutions depend on the parameters. The choice of δ and ε appears to influence which solutions exist, and there seems to be stable solutions hitting one boundary for most choices of parameters.

As pointed out above, the deterministic dynamics of this system are complex and not completely understood. Our approach was to use the methods that are available to obtain some understanding of what is going on. This is far from the rigorous mathematical descriptions available for simpler systems that have been studied for a long time. However, for the study of the stochastically forced system, the obtained understanding was very helpful in interpreting the stochastic results. Also, it was observed that some inferences can be made from the behaviour of the stochastic system back into that of the deterministic version, which was the main motivation behind pursuing this study.

4. The stochastic model

The stochastic model obtained by adding white noise to the r.h.s. of Eq. (9), is written in terms of an SDE for the state space vector process $(\Theta(t), \Phi(t))^{\mathrm{T}}$, where the dimensionless time $\tilde{t}$ has been replaced by t for ease

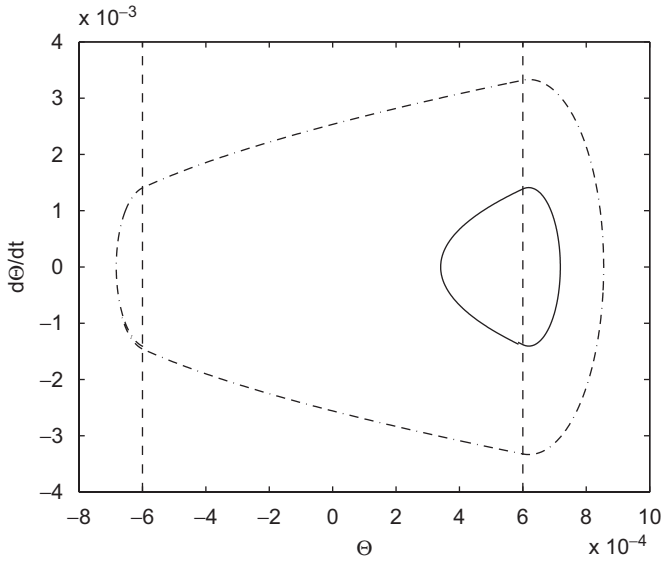

Fig. 3. Phase plots of deterministic solutions for the values of Table 1, $m = 1$ (—) $m = 2$ – –.).

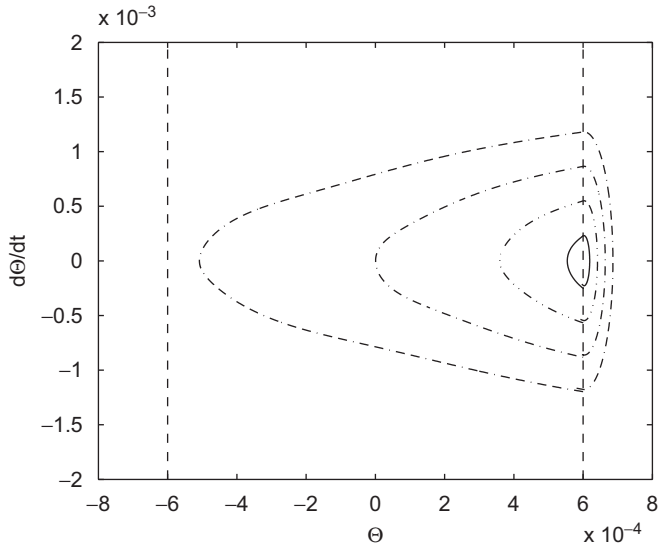

Fig. 4. Phase plots of deterministic solutions for $\delta = 0.5 \times 10^{-4}$. $m = 1$ (—), $m = 2$ (− · ·), $m = 3$ (−·), $m = 4$ (− − ·).

of notation. The superscript T denotes transposition. The SDE obtained can be written as follows:

$$\mathrm{d}\Theta = \Phi \mathrm{d}t,$$

$$\mathrm{d}\Phi = [4\pi\delta - \delta\Phi - 2\kappa B(\Theta)]\,\mathrm{d}t + \varepsilon\cos(2\pi t)\,\mathrm{d}t + \lambda\,\mathrm{d}W(t), \tag{11}$$

where $W(t)$ denotes a standard Brownian motion and λ a parameter for noise strength. The PI algorithm will be the main tool for solving these equations, supported by Monte Carlo simulations.

The added white noise may be considered to serve two purposes. The first is to represent a simple model for physical perturbations to the pure harmonic forcing. The second is to transform the response into a Markov diffusion process, which can be studied by numerical PI.

The previous sections give some information on what qualitative features one may expect. Studying the deterministic system the periodic solutions were seen to be an important element in the dynamics of meshing gears. Based on the general considerations above, the addition of noise is expected to give distributions that show the characteristics of the basins of attraction around these solutions.

As damping is present, it is likely that the effects of the initial condition die out and that a steady state may very well be observed. Due to the sinusoidal forcing, this is expected to be asymptotically periodic.

The SDE (11) has a unique solution in the strong sense for every choice of parameter values, cf. Ref. [20].

5. Path integration

5.1. The basic method

The PI method is based on the fact that the state space vector, $Y = (\Theta, \Phi)^{\mathrm{T}}$, obtained as a solution of the SDE (11) is a Markov vector process. A global solution for the joint PDF $p(y, t)$ of $Y(t)$ as a function of time t is obtained by exploiting the following basic equation:

$$p(y, t) = \int_{\Gamma} p(y, t|y', t')p(y', t')\,\mathrm{d}y', \tag{12}$$

where Γ = state space, $p(y, t|y', t')$ denotes the conditional PDF of $Y(t)$ given that $Y(t') = y'$, $t' < t$. For small time increments $\Delta t = t - t'$, $p(y, t|y', t')$ will be referred to as the incremental transition probability density (TPD) function. For a numerical solution of an SDE, it will be shown that the TPD can always be given as an analytical, closed form expression if the time increment is sufficiently small. Hence, if an

initial PDF, $p_0(y) = p(y, t_0)$ say, is given, then Eq. (12) can be invoked repeatedly to produce the time evolution after t_0 of $p(y, t)$ as follows:

$$p(y,t) = \int_\Gamma \cdots \int_\Gamma \prod_{i=1}^{n} p(y^{(i)}, t_i | y^{(i-1)}, t_{i-1}) \cdot p_0(y^{(0)})\, \mathrm{d}y^{(0)} \ldots \mathrm{d}y^{(n-1)}, \tag{13}$$

where $y^{(n)} = y$, and $t_n = t$.

Eq. (13) expresses the mathematical formulation of the PI principle as adopted here. To arrive at the numerical implementation for the specific dynamic model considered in this paper, let us rewrite Eq. (11) in the following way:

$$\mathrm{d}\,Y(t) = g(Y(t), t)\,\mathrm{d}t + b\,\mathrm{d}W(t), \tag{14}$$

where $g(Y, t) = g(\Theta, \Phi, t) = (\Phi, 4\pi\delta - \delta\Phi - 2\kappa B(\Theta) + \varepsilon\cos(2\pi t))^{\mathrm{T}}$ and $b = (0, \lambda)^{\mathrm{T}}$.

A numerical solution procedure is based on choosing a time increment $\Delta t = t - t'$ such that the PDF of $Y(t)$ can be calculated for each given value of $Y(t')$. The basic version is the Euler–Maruyama approximation of Eq. (14)

$$Y(t) = Y(t') + g(Y(t'), t')\Delta t + b\Delta W(t'). \tag{15}$$

However, as pointed out by Naess and Moe [8], when the deterministic part of the SDE (14) is considered, Eq. (15) reduces to the Euler approximation $y(t) = y(t') + g(y(t'), t')\Delta t$. As is well known, this approximation is only accurate to order $O(\Delta t^2)$. To improve the accuracy, a fourth-order Runge–Kutta (RK) approximation was implemented, which replaced the function $g(y, t)\Delta t$ by the corresponding RK approximation, $\tilde{h}(y, t, \Delta t)$ say, which is written symbolically as $h(y, t)\Delta t$. Naess and Moe [8] then suggested to replace Eq. (15) by what was referred to as the Runge–Kutta–Maruyama (RKM) approximation

$$Y(t) = Y(t') + h(Y(t'), t')\Delta t + b\Delta W(t'). \tag{16}$$

It is realized that in the RKM approximation, the simplest approximation to the integral $\int_{t'}^{t} b\,\mathrm{d}W(s)$ is still retained, viz. $b\Delta W(t')$. Improved approximations to this integral are of course also possible and will lead to yet other approximations beyond Eq. (16) [20]. However, experience indicates that such improved approximations do not substantially improve numerical efficiency for the kind of dynamic systems considered here. In that respect, the most important modification seems to be the implementation of the RK approximation $h(y, t)\Delta t$. This aspect is discusses in more detail in Ref. [8].

Since the Brownian motion process has independent increments, it follows from Eq. (16) that the sequence $\{Y_{n\Delta t}\}_{n=0}^{\infty}$ is a Markov chain. For sufficiently small Δt, it can be shown that this Markov chain will approximate the continuous time Markov process solution of the SDE (5). It is also observed from Eq. (16) that the TPD $p(y, t|y', t')$ is a Gaussian PDF since $\Delta W(t')$ is a Gaussian variable for every t'.

From the assumptions above we may now write the TPD corresponding to Eq. (16)

$$p(y, t|y', t') = \delta(y_1 - y_1' - h_1(y', t')\Delta t) \cdot \tilde{p}(y_2|y', t'), \tag{17}$$

where $y = (y_1, y_2)^{\mathrm{T}}$, $\delta(\cdot)$ denotes the Dirac delta function and

$$\tilde{p}(y_2, t|y', t') = \frac{1}{\sqrt{2\pi\lambda^2\Delta t}} \cdot \exp\left\{-\frac{(y_2 - y_2' - h_2(y', t')\Delta t)^2}{2\lambda^2\Delta t}\right\}, \tag{18}$$

where $h = (h_1, h_2)^{\mathrm{T}}$. Hence, the TPD $p(y, t|y', t')$ is a degenerate multidimensional Gaussian PDF.

5.2. Accurate Runge–Kutta time stepping

An important aspect of the implementation of our PI procedure is a backward RK step, which is done for the deterministic part of the model. By this, all points y' that contribute to the PDF $p(y, t)$ in Eq. (12) are identified, cf. Ref. [8]. For problems of the kind considered in this paper, where the nonlinear restoring force function changes abruptly from the free-play condition to the contact condition with a very stiff restoring

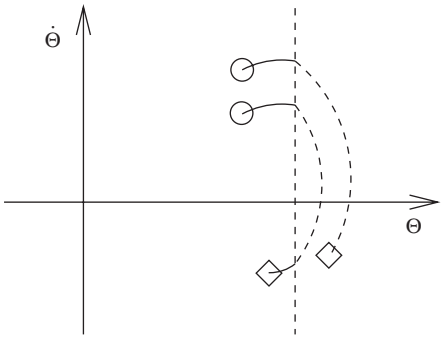

Fig. 5. For the specified time increment Δt a point ○ is mapped by backward time stepping to a point ◇ using a procedure for identifying and separating the contact part of the trajectory (- - -) from the free-play part (−).

force, it becomes important to be able to identify the transition point between the two regimes within a time step Δt. In principle, this can be avoided by using a very small time step, but this is not a practical option. The identification is done by first using an RK-step for the system in the appropriate region combined with a Newton iteration method to locate the transition point on the trajectory. This leads to a time step Δt_1, say. Then a second RK-step over $\Delta t_2 = \Delta t - \Delta t_1$ is used in the other region to locate the correct position of the final point. The requirement to be satisfied is that the time step chosen must allow a sufficiently accurate prediction of all the likely paths in phase space that the system will follow. Fig. 5 shows a schematic of the mapping process. Note that the proper scaling of the discretized noise process is automatically taken care of by the fact that the variance $\mathrm{Var}[\Delta W(t')] = \Delta t$. Hence, changing the time increment automatically changes the variance of the noise variable accordingly.

6. Gear dynamics by path integration

The understanding of the deterministic dynamics provides an idea of the dynamical "landscape" and will be compared to the stochastic behaviour.

First, some initial observations on the behaviour of the PDF are made. In Section 7 the solutions are studied for some interesting choices of parameters. The scope has been limited to parameters in a neighbourhood of the realistic ones.

The PI method provides us with numerical approximations to the probability density function. Drawing conclusions from these can be done only on a qualitative level, still it will be seen that interesting features of the stochastic gear model are observed by studying the PDF.

6.1. Supporting the findings using Monte Carlo simulations

There is, of course, the question of whether the solutions obtained using the PI method really converge towards the correct solution. In order to support the results, they should be compared to the results from Monte Carlo simulations.

It turns out that with the low levels of noise used for studying this system, the strategy of simulating from one initial value and obtaining an average over a long time, did not provide good results. Instead, simulations were run from several initial values and the position at several instants registered.

The results that have been obtained in this manner are neither "dense" nor smooth, but show that the system is indeed attracted towards the same types of solutions found using PI. A couple of examples are shown below.

A RKM-scheme has been used for this. The coefficients are those of the fourth-order explicit RK–scheme with fifth-order time step correction found in Ref. [21, p. 169]. When crossing the boundary, interpolation is performed and integration continued from the boundary into the next domain.

6.2. Initial observations

Before studying the effects of varying parameters in the next sections, a few observations on the overall behaviour of the PDF are made.

A realistic choice of initial values would be inside the free-play region and with reasonable velocities. Choosing an initial distribution centred at the origin with variance so that the mass is mainly inside the free-play region and with the parameters of Table 1, a first observation is made.

The noise strength is chosen small, $\lambda = 1 \times 10^{-5}$, as the scale of the problem is small. The value chosen for this parameter is to some extent arbitrary. However, an investigation into the effect of the noise strength by also using $\lambda = 1 \times 10^{-4}$ and 1×10^{-6}, revealed only a marginal effect. Hence, in this study, we have used $\lambda = 1 \times 10^{-5}$.

It can be seen in Fig. 6 that the solution is drawn towards a PDF that is mainly inside the free-play region and has close resemblance to the $P(m, 1, 0)$-solutions. As the plots are of a qualitative nature the exact values have been omitted, but the blue colour corresponds to low probability density and red to high probability density.

Marginal distributions of position and velocity at two time instants are shown in Fig. 7. The PDF of the position has two peaks, one in the free-play region and one in the impact region. These correspond to low velocities which explains why the system is likely to spend more time there.

Comparing the asymptotic structure to the deterministic trajectories seen in Fig. 4, the similarity to the $P(m, 1, 0)$-solutions seems obvious.

It should be pointed out that the asymptotic distribution is still subject to the periodic forcing and is not a fixed point of the PI operator. This is observed by the peaks of the marginal distributions moving periodically as is illustrated in the velocity plot of Fig. 7. In the following section the average PDF over a period will be used for comparing different solutions.

A Monte Carlo simulation supports the findings from the PI method, but is nowhere near the short run time or the smooth distribution obtained using PI. A plot of the PDF is given in Fig. 8. As can be seen, even for a large number of initial values, the distribution is far from smooth. It does however support the findings in Section 7.

The initial probability density function does obviously influence the time dependent evolution of the PDF, but ideally it should be verified that different choices of PDFs do lead to the same stationary average distribution.

In Fig. 9 an initial PDF with small variance centred well outside the basin of attraction of the $P(m, 1, 0)$ periodic solutions of the deterministic system. The offset PDF of Fig. 9 does spend some time around a $P(m, 1, 1)$-periodic orbit. After ten periods, the snapshot PDF still indicates a $P(m, 1, 1)$-type of solution. To get an impression of the tendency towards a $P(m, 1, 0)$-type solution, which seems to be representative for the long-term picture, 3000 periods were calculated for the initial distributions of Figs. 6 and 9. In Fig. 10 are shown three snapshots of each case: After 1000, 2000 and 3000 periods. This figure reveals two things. Firstly, it appears that for both cases the (instantaneous) PDF will approach the same final PDF. Secondly, even after 3000 periods, the system has not reached its final state.

7. Results

Using the parameters of Table 1 as a point of departure, runs are made to see how the parameters δ and ε affect the average PDF.

The result of varying ε is seen in Fig. 11. For small values, the solutions are not very different. It is only when drastically increasing the eccentricity that a qualitatively different solution is observed.

For $\varepsilon = 0.001$, the bimodal structure of the solution has almost disappeared, suggesting that for large ε stable solutions hitting one side cease to exist. The solution does not, however, have the symmetry in Θ that should be expected from a $P(m, 1, 1)$-structure, suggesting that the underlying deterministic feature is a $P(m, 1, 0)$-orbit that has a minimum close to the lower boundary. This suggests that the familiar $P(m, 1, 0)$-structure of the stationary PDF breaks down for large ε.

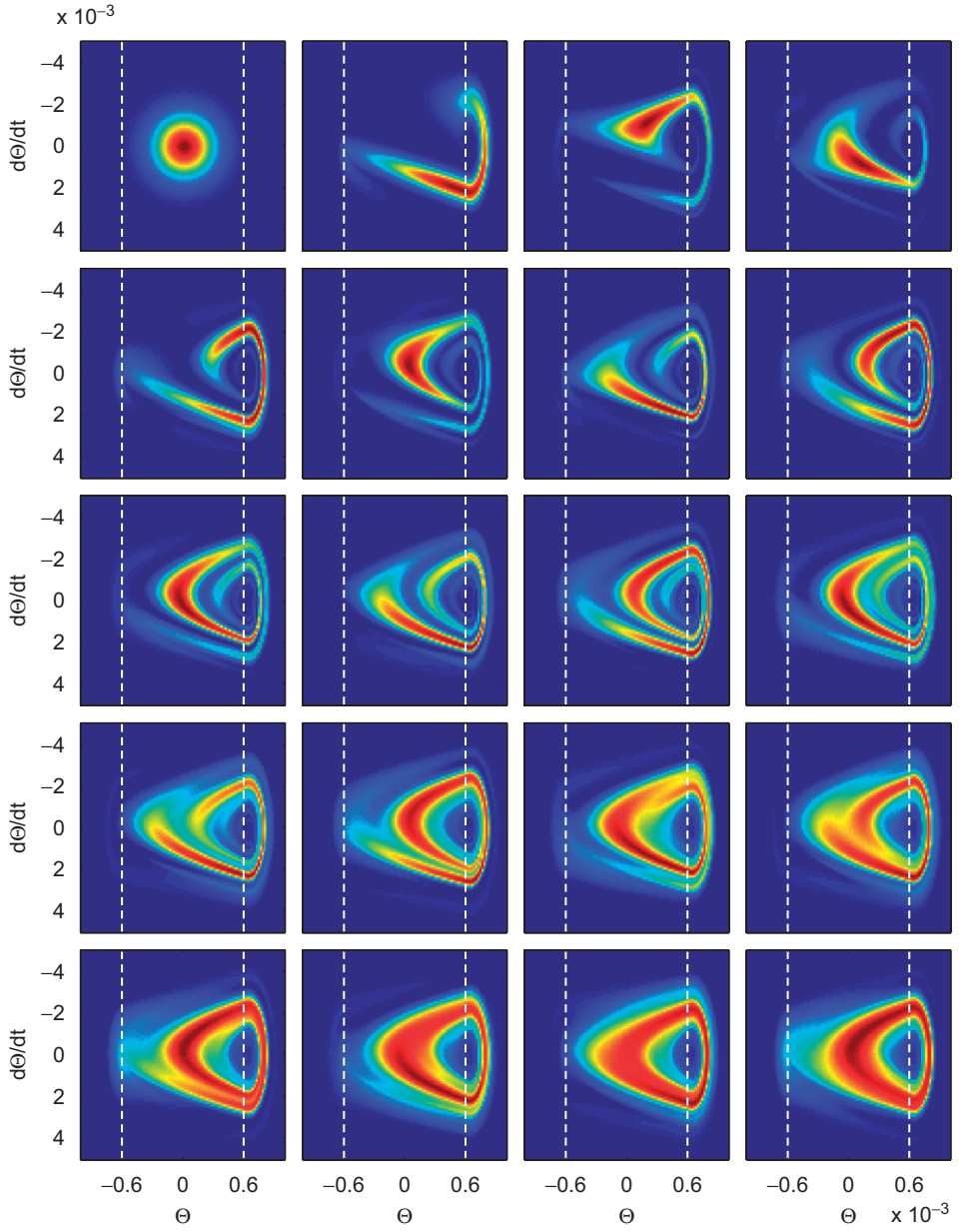

Fig. 6. A path integration result for the stochastic gear model. The time between each snapshot is half a period. Time starts at the upper left hand figure and runs to the right.

Returning to the realistic value of the eccentricity, the damping is varied. From Fig. 12, the value of δ appears to have two functions. As seen when studying the deterministic solutions, the location and existence of solutions seems to depend on the relation between δ and ε. It also appears that δ affects how effectively the probability density is drawn into the potential well. Small δ result in distributions with large tails, large δ give more distinct peaks.

For the largest value of δ used here, the solution has moved across the boundary and it will be seen in the next section that for even larger δ, nearly all the probability mass is found in the upper contact region. When the damping is very low, the resulting distribution is close to a $P(m, 1, 1)$-solution, although there is still a slight asymmetry in favour of the upper contact region.

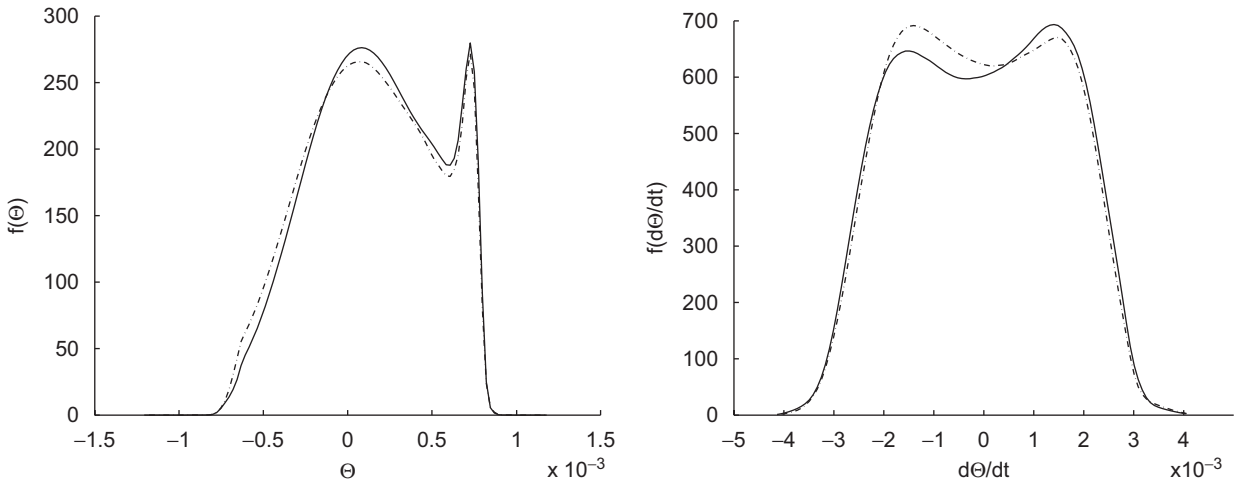

Fig. 7. The marginal distributions of Θ and $\mathrm{d}\Theta/\mathrm{d}t$ at two time instants.

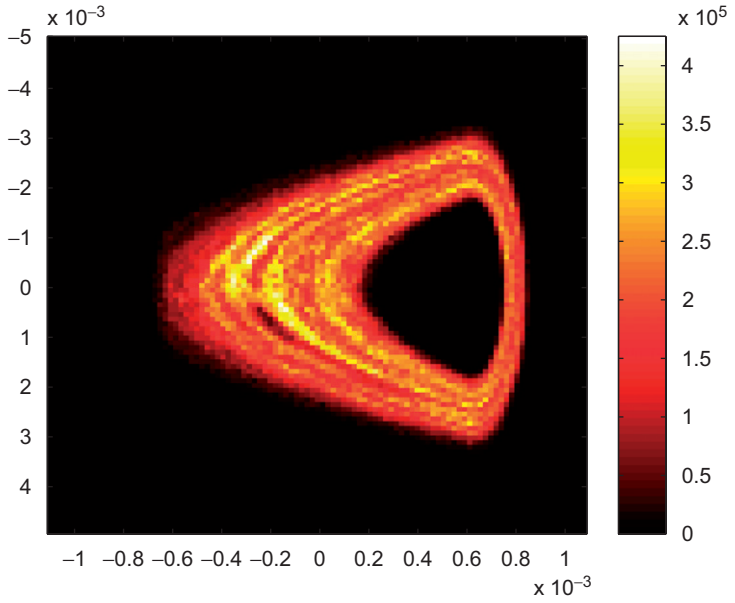

Fig. 8. A Monte Carlo simulation shows a similar structure to that obtained by path integration.

Large eccentricities or small damping increase the time required to reach the stationary state. Such parameter values also give stationary states with very lively periodic behaviour.

It should be emphasized that it appears to be the relation between δ and ε that determines the behaviour, as the PDFs corresponding to realistic ε and low δ show similarities to those for large ε and realistic δ.

8. Summary of observations

The focus here has been on the behaviour of the probability density function for different parameter values and the ability of the PI method to obtain such results.

Choosing different parameters, three classes of solutions have been investigated. The influence of the underlying dynamics is clear, and the stochastic forcing seems to make the system asymptotically stable

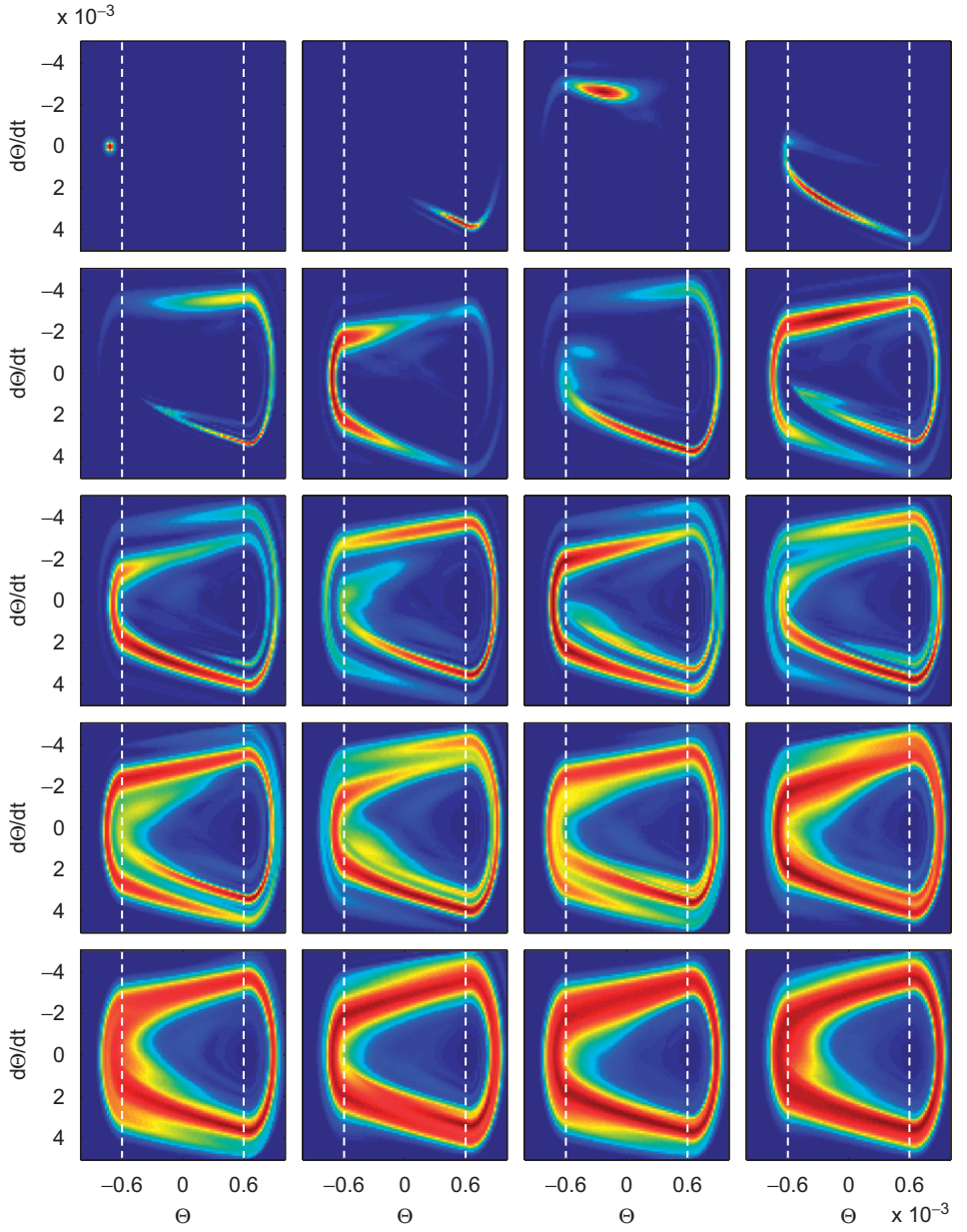

Fig. 9. A narrow initial distribution located close to a $P(m,1,1)$-orbit spreads out, but reflects this kind of solution for some time. However, the solution converges eventually towards a PDF that reflects a $P(m,1,0)$-solution. The time between snapshots is still half a period.

revealing important aspects of the dynamics, especially concerning the stability of periodic solutions. Compared to classifying solutions for the deterministic case which is a hard problem to solve, adding noise and observing the PDF provides a "map over the deterministic landscape" in an elegant manner.

If the situation where the system is in permanent contact is considered optimal and a state hitting one side is considered to be behaving nicely, the overall impression is that high values of the relation δ/ε result in well behaving systems.

The suggestion to minimize the eccentricity is, perhaps, not as surprising as the idea of increasing the damping. While the first requires an increased accuracy in the manufacturing that may be hard to obtain, the

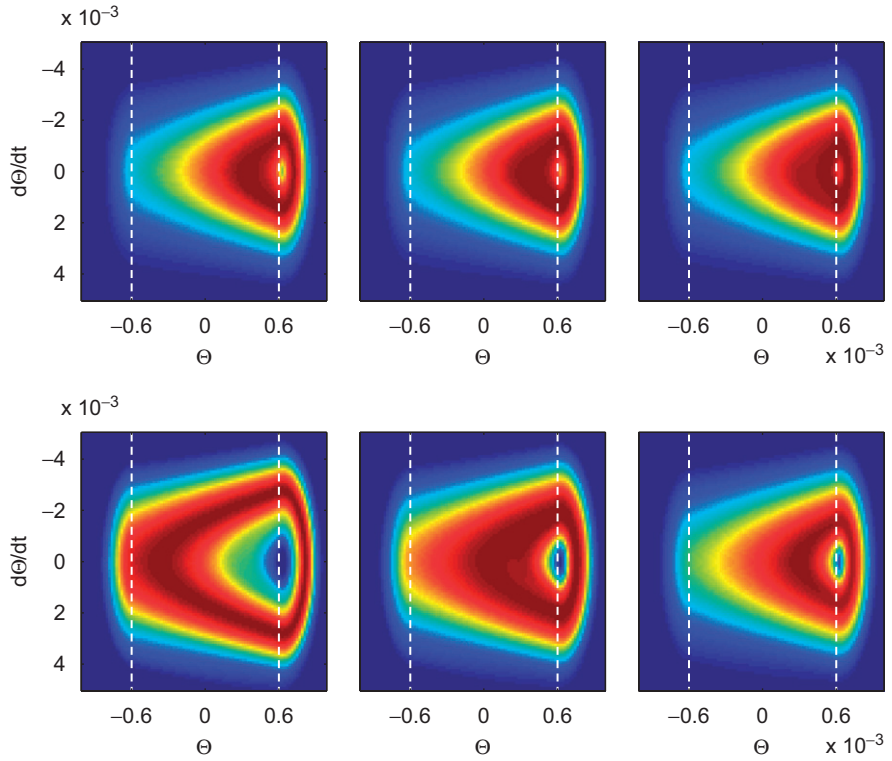

Fig. 10. Snapshots of the PDF at 1000, 2000 and 3000 periods. The upper row corresponds to the initial PDF of Fig. 6, while the bottom row corresponds to the initial PDF of Fig. 9. The number of periods is increasing from left to right.

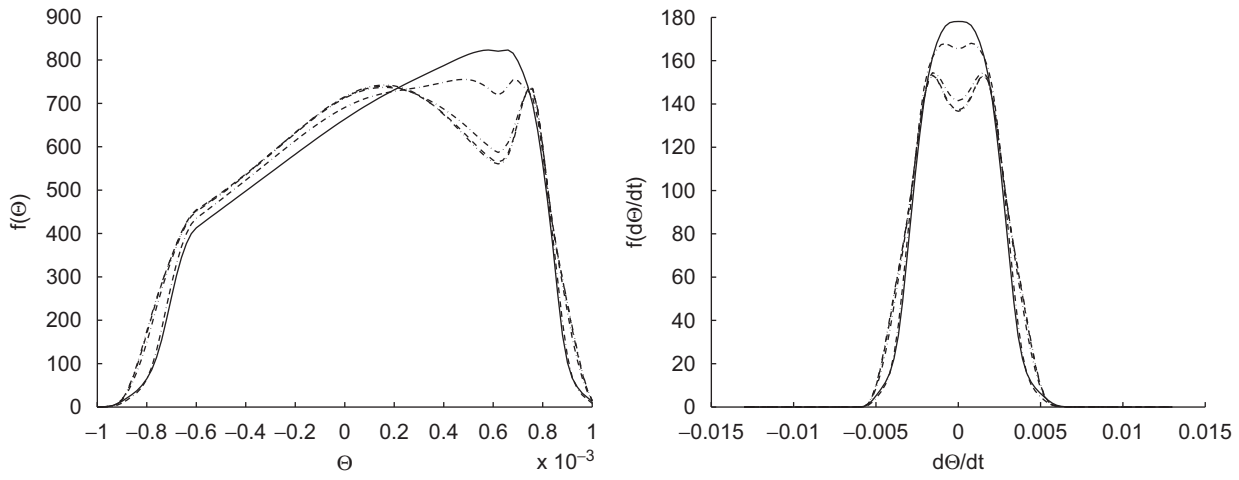

Fig. 11. Marginal distributions of Θ and $\mathrm{d}\Theta/\mathrm{d}t$ for different values of $\varepsilon \cdot \varepsilon = 1.0 \times 10^{-5}$ $(- \cdot \cdot)$, $\varepsilon = 5.0 \cdot 10^{-5}$ $(--)$, $\varepsilon = 1.0 \times 10^{-4}$ $(-\cdot)$, $\varepsilon = 5.0 \times 10^{-4}$ $(- - \cdot)$ and $\varepsilon = 1.0 \times 10^{-3}$(—).

second is easily obtained by increasing the friction. The system will, of course, be less efficient, but this might not be a significant loss. As the real–life geared system is subjected to random perturbations, these observations are believed to be of interest when designing such systems.

PI seems to deal with piecewise linear systems in an excellent manner. Applied in its original form, the solutions are convincing, but an adaptation of the method to improve the accuracy for piecewise linear problems has been suggested and used to obtain the results above.

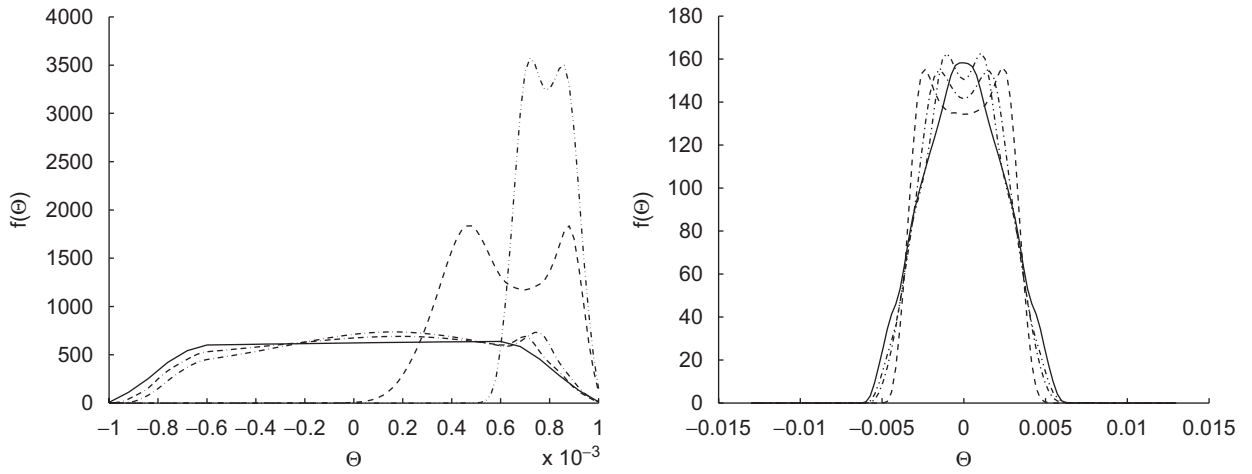

Fig. 12. Marginal distributions of Θ and $\mathrm{d}\Theta/\mathrm{d}t$ for different values of δ. $\delta = 3.0 \times 10^{-3}$ $(- \cdot \cdot)$, $\delta = 1.5 \times 10^{-3}$ $(- -)$, $\delta = 3.0 \times 10^{-4}$ $(- \cdot)$, $\delta = 1.5 \times 10^{-4}$ $(- - \cdot)$ and $\delta = 3.0 \times 10^{-5}$(—).

9. Concluding remarks

The main purpose of this work has been to investigate the potential applicability of numerical path integration to the study of the dynamics of meshing gears. Even though the nonlinearity of the dynamic model poses a challenge in the implementation of numerical path integration, it appears that the method can indeed serve as a very useful additional tool for the study of such systems. Applying the method to the specific model at hand has revealed several interesting features and lead to a deeper understanding of the dynamics of the system.

In this paper we have wanted to study the deterministic dynamics of a pair of meshing gears. To make available the path integration technique, a small amount of white noise was added. The intensity of the white noise is largely arbitrary as long as it is small enough to avoid noticeable effects on the dynamics of the system. This is simply checked by varying the intensity over a range of, say, two orders of magnitude, which was done for the model used in this paper.

A final comment may be appropriate. It is often poorly understood, or not fully appreciated, that the numerical path integration method in fact provides the complete solution to the dynamics of the approximate model under study. Approximate in the sense of a numerical solution of Eq. (16) with specified initial conditions. Within this framework of discretization and smoothing by interpolation, the whole dynamic picture is present. If one knows how to interpret the joint probability density function of the state space process, a unique insight into the dynamics of the system is at hand.

Acknowledgements

One of the authors, F. E. Kolnes, would like to express his gratitude to Drs. E. Wilson and M. Homer at University of Bristol for their hospitality and guidance on the deterministic dynamics of gear systems during his extended visit at UB in 2004. The authors would also like acknowledge the Research Council of Norway for supporting part of this work.

References

[1] A. Kubo, K. Yamada, T. Aida, S. Sato, Research on ultra high speed gear devices, *Transactions of the Japan Society of Mechanical Engineers* 38 (1972) 2692–2715.

[2] K. Umezawa, T. Sata, J. Ishikawa, Simulation of rotational vibration of spur gears, *Bulletin of the Japanes Society of Mechanical Engineers* 27 (1984) 102–109.

[3] A. Kahraman, R. Singh, Non-linear dynamics of a spur gear pair, *Journal of Sound and Vibration* 142 (1) (1990) 49–75.
[4] A. Parey, N. Tandon, Spur gear dynamic models including defects: a review, *Shock and Vibration Digest* 35 (6) (2003) 465–478.
[5] J. Wang, R. Li, X. Peng, Survey of nonlinear vibration of gear transmission systems, *Applied Mechanics Reviews* 56 (3) (2003) 309–329.
[6] K. Sato, S. Yamamoto, O. Kamada, N. Takatsu, Jump phenomena in gear system to random excitation, *Bulletin of the Japanese Society of Mechanical Engineers* 28 (1985) 1271–1278.
[7] A. Naess, J.M. Johnsen, Response statistics of nonlinear dynamic systems by path integration, in: F.C.N. Bellomo (Ed.), *Proceedings of the IUTAM Symposium on Nonlinear Stochastic Dynamics*, Berlin, Springer, 1991, pp. 401–414.
[8] A. Naess, V. Moe, Efficient path integration methods for nonlinear dynamic systems, *Probabilistic Engineering Mechanics* 15 (3) (2000) 221–231.
[9] A. Kunert, F. Pfeiffer, Stochastic model for rattling in gear boxes, *Proceedings of the IUTAM Symposium on Nonlinear Dynamics in Engineering Systems*, 1989, pp. 173–180.
[10] F. Pfeiffer, A. Kunert, Rattling models from deterministic to stochastic processes, *Nonlinear Dynamics* 1 (1990) 63–74.
[11] C. Halse, R. Wilson, M. Homer, M. di Bernardo, Coexisting solutions and bifurcations in mechanical oscillators with backlash, Preprint, University of Bristol, 2006.
[12] R.G. Parker, S.M. Vijayakar, T. Imajo, Non-linear dynamic response of a spur gear pair: modelling and experimental comparisons, *Journal of Sound and Vibration* 237 (3) (2000) 435–455.
[13] S. Theodossiades, S. Natsiavas, Periodic and chaotic dynamics of motor-driven gear-pair systems with backlash, *Chaos, Solitons and Fractals* 12 (2001) 2427–2440.
[14] G. Litak, M.I. Friswell, Dynamics of a gear system with faults in meshing stiffness, *Nonlinear Dynamics* 41 (2005) 415–421.
[15] C. Padmanabhan, R. Singh, Dynamics of a piecewise non-linear system subject to dual harmonic excitation using parametric continuation, *Journal of Sound and Vibration* 184 (5) (1995) 767–799.
[16] M.F. Dimentberg, D.V. Iourtchenko, Random vibrations with impacts: a review, *Nonlinear Dynamics* 36 (2004) 229–254.
[17] V.I. Babitsky, V.L. Krupenin, *Vibration of Strongly Nonlinear Discontinuous Systems*, Springer, Berlin, 2001.
[18] R.I. Zadoks, A. Midha, Parametric stability of a two-degree-of-freedom machine system part I—equations of motion and stability, *Journal of Mechanisms Transmissions and Automation in Design* 109 (1987) 210–215.
[19] A. Kahraman, R. Singh, Interactions between time-varying mesh stiffness and clearance non-linearities in a geared sytem, *Journal of Sound and Vibration* 146 (1) (1991) 135–156.
[20] P.E. Kloeden, E. Platen, *Numerical Solutions of Stochastic Differential Equations*, Springer, New York, 1992.
[21] E. Hairer, S. P. Nørsett, G. Wanner, *Solving Ordinary Differential I—Nonstiff Problems*, Springer, New York, 1987.